# NEUTRON AND NEUTRON-INDUCED GAMMA RAY SIGNATURES AS A TEMPLATE MATCHING TECHNIQUE FOR EXPLOSIVES DETECTION

by

REBECCA L. BREWER

B.S., Kansas State University, 2005

---

A THESIS

submitted in partial fulfillment of the
requirements for the degree

MASTER OF SCIENCE

Department of Mechanical and Nuclear Engineering
College of Engineering

KANSAS STATE UNIVERSITY
Manhattan, Kansas
2009

Approved by:

Major Professor
William L. Dunn, Ph.D.

## ABSTRACT

Improvised explosivse devices (IEDs) are the cause of many casulaties worldwide. Current methods for detecting IEDs are insufficient. A signature-based scanning technique based upon the fact that explosives consist primarily of hydrogen, oxygen, nitrogen, and carbon is examined as a possible rapid, standoff method for detecting IEDs. Devices employing this method rely on a template-matching technique in which the detector responses acquired through neutron and photon interrogation are compared to responses from a known explosive. A figure-of-merit is calculated to determine how well the template and the unknown match. This thesis explores the feasibility of employing the neutron interrogation aspect of this method.

# Table of Contents

# List of Figures

# List of Tables

# Acknowledgments

The author would like to express gratitude to the many people who aided in the completion of this thesis. The author would, in particular, like to thank Dr. William L. Dunn for his continuous support and encouragement throughout the completion of this thesis. He always believed the author could complete this project even when she was unsure of her abilities to do so.

The author also thanks Dr. J.K. Shultis and Dr. Kevin B. Lease for serving on her supervisory committee. She is also grateful for the contributions of David Vu, Xianzhi Yang, Justin Lowrey, Clell J. Solomon, Jr., Ryan Green, Lisa Kitten, Joshua Van Meter, Cristi Pedotto, Dominic Pedotto, Tom Dunn, and the K-State TRIGA Mark II Reactor Staff.

This research was supported in part by M2 Technologies, Inc., Contract No. M67854-02-D-1110 Task 1/8/11 from the United States Marine Corps System Command, and the National Academy for Nuclear Training Fellowship Program.

# Chapter 1

# Introduction and Background

## 1.1 Introduction

Improvised explosive devices (IEDs) caused 2,398 deaths and 22,378 injuries to members of the United States military during the Global War on Terrorism between October 7, 2001 and April 4, 2009 [1]. In addition, numerous bystanders have been injured or killed. Many of these explosive devices are hidden and detonated in automobiles. Currently, vehicles entering military bases, embassies, and other similarly access-controlled locations are checked for explosives by physical search, x-rays, or scent dogs [2]. Physical searches are time consuming and could be unsafe for the searcher. X-rays are inconclusive when used on vehicles because their primary function is to detect metals, which make up a significant portion of an automobile. Scent dogs can be unreliable and get tired after several searches. One can only conclude that current methods of detecting explosives are insufficient. Thus, it is necessary to create a rapid, non-intrusive system for detecting explosives if the number of casualties due to IEDs is to be reduced.

## 1.2 System Requirements

An explosive device consists of three primary components: an explosive, a detonator, and packaging. Historically, detection has been based upon detecting the packaging because it often is metal. Recently, it has become more common to use wood or plasitc for the packaging [3]. Therefore, detecting the packaging has become an unreliable method. Detection

methods based upon finding the explosive and/or detonator must be developed. This project focuses on detecting the explosive.

The most commonly used explosives consist primarily of hydrogen, oxygen, carbon, and nitrogen. Further, the fraction of an explosive's molecules consisting of nitrogen and oxygen is high and the fraction consisting of carbon and hydrogen is low. In addition, the density of an explosive typically ranges from 1.2 to 2.0 grams per cubic centimeter [4, 5], which is greater than the density of most organic materials but less than the density of most metals [6]. Therefore, a successful explosives detection system will be able to not only identify the presence of hydrogen, oxygen, carbon, and nitrogen, but also determine the ratio of one element's composition to another's. The system should also have a low false alarm rate and be able to detect the presence of an explosive material with other inert materials present.

Nuclear-based methods, particularly neutron interrogation, are useful because the elements hydrogen, oxygen, carbon, and nitrogen vastly differ in their modes of interaction with neutrons. These differences allow researchers to determine which of these elements are present. Neutrons are a beneficial method of interrogation because they penetrate an object one to two meters without much attenuation, even steel casings [7–9]. This allows a neutron interrogation system to be non-intrusive, i.e, a package or vehicle can be examined without having to unpack it. Additionally, electromagnetic forces have no impact on neutrons so they interact only with nuclei, which contributes to their large penetration ability.

Neutron sources are readily available as radioisotope sources and as neutron generators. Neutron generators accelerate nuclear particles that are used to bombard deuterium, tritium, or beryllium. The particles react with a target to produce neutrons. Most radioisotope sources and generators are portable. However, sources cannot be turned "on" and "off" as can neutron generators, which makes generators safer when not in use.

An interrogation system must also meet strict safety standards. Neutrons are particularly hazardous and must be properly shielded. The user must also be safe, so a system that can be operated remotely is desired. It must also be constructed so that if an accident were to occur, little or no radiation would be released.

Finally, the system must rapidly interrogate an unknown and quickly analyze the results.

The entire process should take only a few minutes.

## 1.3 Neutron Interactions

Neutrons are either scattered or absorbed. In scattering, a neutron collides with a nucleus and loses an element-dependent amount of energy. The nucleus is either left in the ground state but with additional kinetic energy (elastic scattering) or in an excited state (inelastic scattering). In inelastic scattering, the nucleus usually returns to the ground state by emission of an inelastic scatter gamma ray, as illustrated in Figure 1.1. When a neutron is absorbed a compound nucleus in an excited state often results. The excited nucleus returns to the ground state by emitting one or more capture gamma rays, as illustrated in Figure 1.2. These gamma rays are characteristic of the target nucleus. Other absorption interactions lead to emission of neutrons, protons, deuterons, or other charged particles including fission fragments.

## 1.4 Device Operation Principles

Signature-based interrogation relies on a template-matching technique. Detector responses are acquired through neutron and photon interrogation of an unknown object and are compared to a "template" consisting of detector responses that are typical of those from a known explosive. Then, a figure-of-merit is calculated to determine how well, statistically, the template matches the unknown and the figure-of-merit serves as an indication of the probability that the unknown object contains an explosive. A database of explosive templates will be created for different types of packaging. This method differs from many other interrogation techniques in using both photon and neutron interrogation, which provides more information than using either individually. The research discussed in this thesis focuses on the neutron interrogation portion of the explosives identification method.

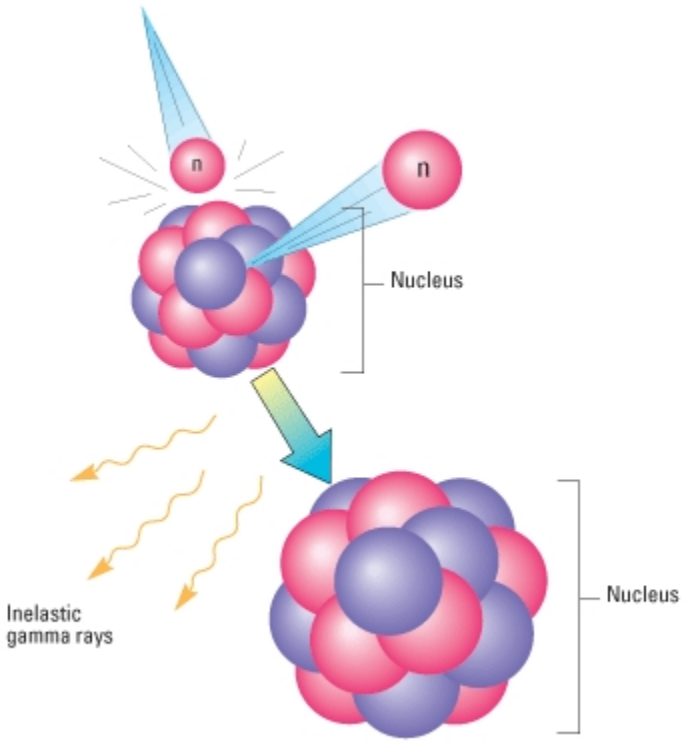


**Fig. 1.1.** Inelastic Neutron Scattering
(from http://www.glossary.oilfield.slb.com/DisplayImage.cfm?ID=644)

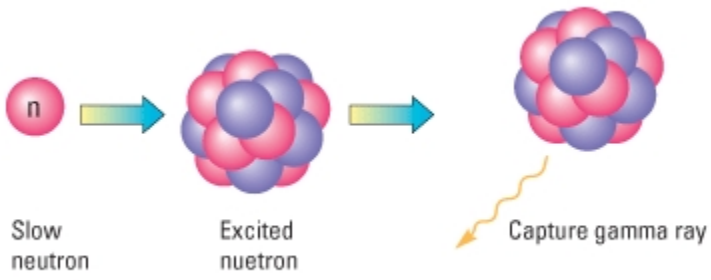


**Fig. 1.2.** Neutron Absorption
(from http://www.glossary.oilfield.slb.com/DisplayImage.cfm?ID=645)

# Chapter 2

# Existing Explosive Detection Methods

There are currently a wide variety of methods for detecting explosives. Some work better than others and some are applicable to certain specific situations. Several methods are discussed below.

## 2.1 Metal Detectors

A rudimentary method of detecting explosives is use of the metal detector. It is comprised of a coil that generates a magnetic field [3, 10] that is disturbed by metal objects. Although light weight [10], this device is unreliable. It can only be used to detect explosives encased in metal. In addition, metal detectors cannot be used to detect explosives within most vehicles because metal components of the vehicle would result in too many false positives.

## 2.2 X-Ray Radiography

Sometimes called Roentgenography [11], x-ray radiography depends on the absorption coefficients and atomic numbers of the elements in an object. This type of system does not actually detect explosives, but rather explosive-like characteristics. Advantages of x-ray radiography are that it is safer for humans and objects being tested than other methods [12], it is a well understood method, and it is inexpensive compared to neutron-based methods. X-ray machines are reasonably sized [4, 5], have a ten to fifteen foot standoff potential [13], and x-ray devices are acceptable to the general public. A major disadvantage is the depenence upon a human to interpret an image properly. Since explosives can be molded into

infinitely many forms, they cannot be recognized by shape. Objects of similar density appear identical and high density objects can obscure lower density objects. Typically, x-ray systems have a high false positive rate due to these shortfalls. In addition, the elements hydrogen, oxygen, nitrogen, and carbon, of which the majority of explosives are primarily composed, have low interaction probabilities with x radiation [4, 5]. Four specific types of radiography are discussed below.

### 2.2.1 Transmission Radiography

Also called conventional or single-energy x rays, this method measures how much an x-ray beam is attenuated after passing through the object in question. An image of the object is created in which the areas where the beam is less intense appear darker. In this system, a thin strong absorber and a thick weak absorber appear identical. [12] Although images are produced with a high resolution [13], they are only indicative of bomb parts such as fusing, wiring, and metal and not of explosives themselves [14]. The detector and source are required to be on opposite sides of the object in question [13]. The images produced via transmission x rays do not provide enough information for the detection of explosives.

### 2.2.2 Dual-Energy Radiography

The object is scanned at two energy levels, e.g., once at about 80 kV and once at above 100 kV. At the lower energy level, the absorption is dependent upon the thickness and atomic number of the object material. At the higher energy absorption is dependent on density. [12] A transmission image is created at each energy and the two images are compared to determine if explosives are present [12, 14]. Carbon, nitrogen, and oxygen are dark in the low energy image, but not in the high energy image [12]. The false positive rate of this type of system is roughly twenty percent [15].

### 2.2.3 Backscatter Radiography

An image from the x rays reflected back toward the x-ray source (backscatter image) is created and in addition another image may be created via the transmission method described

above (forward scattering image) [12, 14]. The backscatter image is dependent upon how much energy is absorbed during forward scattering, how much energy is backscattered, and how many x rays reach the backscatter detectors [12]. Hydrogen, oxygen, carbon, and nitrogen are more efficient at scattering x rays and therefore stand out more (are darker) on backscatter images while they are barely visible in transmission images [9]. Both the forward scatter and backscatter images are affected by the object's placement in relation to the x-ray source and the detectors [12]. Although the resolution of images generated via this method is not as good as images produced via transmission x rays, backscatter x rays give more information than transmission x rays [13] since the forward scatter image provides information on high density materials and the backscatter image provides information on organic materials [14].

### 2.2.4 Computed Tomography

In tomographic imaging, images are constructed from the transmission of photons through an object. The image is a function of the object's attenuation coefficient(s). [11] The sources and detector are rotated around the object so a cross-sectional image of the object can be obtained. The cost of operating a computed tomography system is high [12, 14] and the system results in a higher radiation dose than x-rays and therefore requires more shielding [9, 14]. It can be difficult and time consuming to obtain transmission measurements of a target at many angles. The data analysis is also a time-consuming process [13].

## 2.3 Spectroscopy

In spectroscopic analysis, a small sample of the object in question is burned and the light emitted is dispersed through a prism. The color and thickness of the spectral lines is characteristic of the composition and density of the object. [11] Obviously, this method cannot be used on an explosive device as the explosive would detonate when burned.

## 2.4 Nuclear Magnetic Resonance

Nuclear Magnetic Resonance (NMR) imaging uses radiofrequency photons. The object is placed in a strong magnetic field in which radiofrequency photons are absorbed by neutrons. The neutrons then de-excite by releasing a photon of almost the same energy as the original photon. The material of an object can be identified because different elements absorb radiofrequency photons of different frequencies. Only elements with odd numbers of protons can be imaged because pairs of protons and neutrons cancel one another out. [11] Additionally, since a high-powered magnet is used, NMR cannot be applied to objects containing or encased in metal [6].

## 2.5 Neutron Activation Analysis

The object is bombarded with neutrons and results in the production of radioactive isotopes. Whereas an object can be moderated by neutrons and the residual gamma rays emitted by radioisotopes can, in principle, be used to identify the nuclides present, this technique is not good for explosives detection because the half lives of nuclides vary considerably and the elements typically found in explosives do not produce many radioisotopes.

## 2.6 Thermal Neutron Activation

The primary objective of a thermal neutron activation (TNA®) system is to identify nitrogen, usually via detection of the 10.83-MeV capture gamma ray from $^{14}$N. Neutrons produced by a radioisotope source or a neutron generator are moderated (thermalized) to thermal energies that average about 0.025 eV. The thermal neutrons then bombard the object in question and a fraction of the neutrons are absorbed by the nuclei of the elements within the object. The nuclei de-excite by emitting prompt gamma rays of energy characteristic of the nuclei. This system can only be used to determine if an element such as nitrogen is present, not for what use it is intended, i.e., the results of analysis are the same for an explosive containing nitrogen and a fertilizer containing nitrogen. Due to this characteristic, there can be a high false positive rate [12, 14]. This method has limited sensitivity and can

be quite expensive [12, 14]. It also must be corrected for background created by thermal neutron interactions with shielding, detectors, and surrounding materials. It cannot be used to identify carbon or oxygen [16, 17], and is slow compared to other neutron interrogation methods [10, 16]. TNA® can be used to detect as few as 200 g of explosive material [12], but is unable to interrogate large targets due to the limited penetration ability of thermalized neutrons.

## 2.7 Fast Neutron Analysis

Fast Neutron Analysis (FNA) identifies not only nitrogen, as in the TNA® method, but also hydrogen, oxygen, and carbon. It uses high energy fast neutrons, usually from a neutron generator, to excite nuclei via inelastic scattering and the nuclei de-excite by releasing characteristic gamma rays. The gamma rays are detected by several detectors surrounding the object in question [18, 19]. The intensity of the gamma rays is indicative of the amount of an element within an object while the energy is indicative of the type of element. The intensity can be used to calculate elemental ratios. [9] However, the use of high energy neutrons causes a high background in the gamma ray detectors which skew the results. This method does not require the use of moderators, as in TNA®, which makes the system have less mass and be more portable [6]. More complex than TNA®, FNA provides more accurate results [9, 10].

## 2.8 Pulsed Fast Neutron Analysis

Pulsed Fast Neutron Analysis (PFNA®) is similar to FNA, except the neutron source is pulsed instead of a constant stream in an attempt to reduce the high gamma ray background that occurs in FNA. The neutron pulses are usually nanoseconds long and must be as monoenergetic as possible in order to ensure that all neutrons travel at identical velocities [9, 10, 20]. Pulses are usually about 8 MeV [5, 21]. The neutrons produce gamma rays through inelastic scattering and the gammas are detected with an array of thallium doped sodium iodide (NaI(Tl)) detectors [5, 20]. The time from the start of the neutron pulse to the detection of a gamma ray is measured. This allows for the determination of not only

elemental composition of the object, but also the spatial location of the elements within the object. One major setback to PFNA® is that it is difficult to create an efficient high energy pulsed neutron source that can be safely operated and is cost effective [10, 12]. However, PFNA® devices have a false positive rate of less than five percent [12].

## 2.9 Pulsed Fast Neutron Transmission Spectroscopy

First used by Overly [20, 22], nanosecond pulsed beams of neutrons attenuate when passing through an object [23, 24]. The neutron beam energy is measured before and after transmission [20]. A pulsed fast neutron transmission spectroscopy (PFNTS) system is costly, heavy, and can be unsafe [5]. Since this is a transmission method, it requires that the object be between the source and detector [6].

## 2.10 Pulsed Fast/Thermal Neutron Analysis

Pulsed fast/thermal neutron analysis (PFTNA) is essentially a combination of the TNA® and PFNA® methods. A neutron generator produces a beam of microsecond long pulses and the resulting inelastic scatter gammas are measured. After a series of pulses, the generator is turned off for approximately 100 microseconds and prompt gammas from the capture of thermal neutrons are measured [9, 10, 25]. This system usually employs a bismuth germanate (BGO) or gadolium ortho-silicate (GSO) detector [25]. The data acquisition can be performed in as few as thirty seconds [25], but as with any system, the longer the data acquisition time, the more accurate the measurement.

## 2.11 Neutron Backscattering

The objective of neutron backscattering (NBS) is to determine hydrogen content within an object [26–28]. It is based upon the principle that explosives contain a higher concentration of hydrogen than inert materials [27, 28]. The method was introduced in 1999 by F.D. Brooks with the intended application of detecting land mines [27].

An object under question is interrogated by bombarding it with a beam of fast neutrons. Neutrons scattered and thermalized by the object are then detected with a thermal neutron detector. If hydrogen is present, the neutrons will undergo more moderation than in non-hydrogenous materials resulting in a higher thermal neutron flux in the hydrogenous material. An NBS system quickly scans an object for explosives. It is insensitive to metals, which allows for the detection of explosives that do not contain metal and for application in detecting explosives in automobiles. However, moisture content of the atmosphere impacts the effectiveness of the system - a high moisture content causes hydrogen rich materials to be indistinguishable from the atmosphere. In addition, false positives can result from inert hydrogen rich materials such as water and plastics [27].

## 2.12 Fast Neutron Scattering Analysis

A monoenergetic neutron beam alternating between two energies bombards an object in question [4, 5, 29]. Neutrons scattered by the object are detected at forward and backward angles as shown in Figure 2.1 [4, 5, 24]. The type, number, intensity, and scattering angle of the neutrons are characteristic of the elements composing the object [4]. An explosives signature is created by combining measurements from the two detectors [4, 5].

## 2.13 Associated Particle Imaging

Associated Particle Imaging (API) uses the alpha particle from the $^{3}H(d,n)^{4}He$ reaction in the production of 14-MeV neutrons to "tag" the neutron. A 3.5 MeV alpha particle is emitted at the same time as and $180^{o}$ from each 14-MeV neutron. The tagging of the neutron allows for close monitoring of the neutron's direction, which allows for spatial mapping without a pulsed neutron beam. As in FNA and PFNA®, the characteristic gamma rays are used to determine the elemental composition of the object. [5, 6, 30]

## 2.14 Nuclear Quadruple Resonance

Nuclear Quadruple Resonance (NQR) detects the electric quadrupole moment in $^{14}$N [6, 10]. A radiofrequency signal is applied to the object in question [10, 14] moving $^{14}$N to a higher energy state [14]. If $^{14}$N is present, a radio signal will be produced when the radiofrequency signal is removed [10]. The radio signal is unique to $^{14}$N and can be detected with a radio receiver [8, 10]. This method produces no ionizing radiation [14] which makes it safer than most of the other methods detailed in this chapter. However, the radio signal is usually weak which means the target must be in close proximity to the radiofrequency field, therefore, this method can only be used on small items [14]. In addition, the radio signal can be indistinguishable from electronic noise [6] and the system is expensive and requires large amounts of power [31].

## 2.15 Projects Employing Methods

### 2.15.1 Improved Landmine Detection System

The Canadian Department of National Defense (DND) in conjunction with General Dynamics Canada (GDC) created a multisensor system to detect landmines after concluding that no single detection method could successfully determine the presence of a landmine [16]. This system, called the Improved Landmine Detection System (ILDS) employs an electromagnetic induction metal detector, a ground probing radar, and a forward-looking infrared imager as primary detection methods in the first vehicle [10, 16]. If a landmine is suspected, a TNA® system housed in a second vehicle is then used as a secondary detection method [10, 16, 32]. An illustration of the system can be found in Figure 2.2. This TNA® system is based upon detection of the 10.83-MeV prompt gamma from nitrogen. The DND chose to only look at the single prompt gamma because there are few competing gammas at that energy, nitrogen has a relatively high thermal neutron capture cross-section, and a thallium doped sodium iodide (NaI(Tl)) detector can be used instead of a bulkier germanium detector. The system is equipped with a $10^8$ neutrons per second $^{252}$Cf source, four 3x3 NaI(Tl) detectors at ninety degree intervals, and a source to detector distance of 30 cm. This system was found to be

able to detect landmines within a 1200 $cm^2$ radial area and nitrogen concentration as low as 100 grams in as little as five minutes. [32]

### 2.15.2 Delft University Neutron Backscattering Imaging Detector

The Delft University Neutron Backscattering Imaging Detector (DUNBID) employs neutron backscattering to detect explosives [27]. It consists of 16 parallel $^3$He proportional counters in a 80 cm by 70 cm by 7 cm box [10, 27]. The detectors are made of aluminum, are 50 cm long, and are 2.5 cm in diameter. A 0.5 mm cadmium sheet is on top of the detectors to filter out slow neutrons. The neutron source is a 7000 neutron per second $^{252}$Cf source placed in the center of the detector array. [27] The entire apparatus weighs approximately 10 kg [27] and is mounted on a remote control vehicle [10].

### 2.15.3 Delft University Neutron Backscattering Landmine Detector

The Delft University Neutron Backscattering Landmine Detector (DUNBLAD) was developed by the same team that developed the DUNBID. The DUNBLAD employs both metal detection and neutron backscattering. The DUNBLAD uses eight 50 cm long, 2.54 cm diameter $^3$He detectors divided into two groups of four placed 18 cm apart and a $^{252}$Cf source between the two sets of four detectors. The downside to using the $^{252}$Cf source is that it cannot be turned off. The DUNBLAD would need to be constructed so that if an accident were to occur, no additional radioactive material would be released. However, the advantage of the neutron source over a neutron generator is that the neutron source can be carried by a person while a neutron generator would need to be on a cart or wheeled platform. [28]

The neutron backscatter and metal detector apparatuses are encased in polychlorotrifluorethylene, a plastic containing no hydrogen. The DUNBLAD has two 1.5 m carbon fiber poles and is carried by a person as shown in Figure 2.3. The weight of the detector is balanced by batteries, which will run up to eight hours. The detector is workable but would ideally be lighter as it weighs approximately 18 kg. It also does not work very well on uneven terrain. [28]

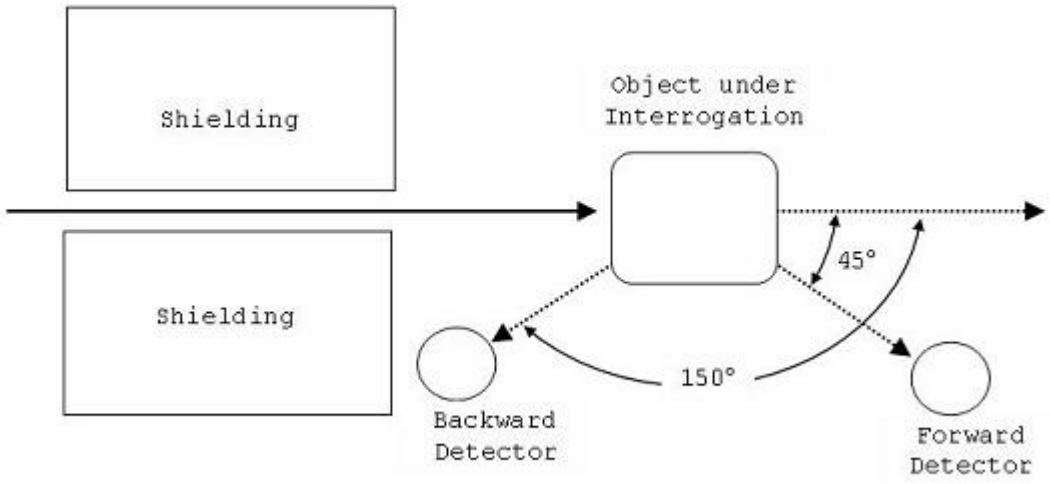


**Fig. 2.1.** FNSA Schematic
(Adapted from [4])

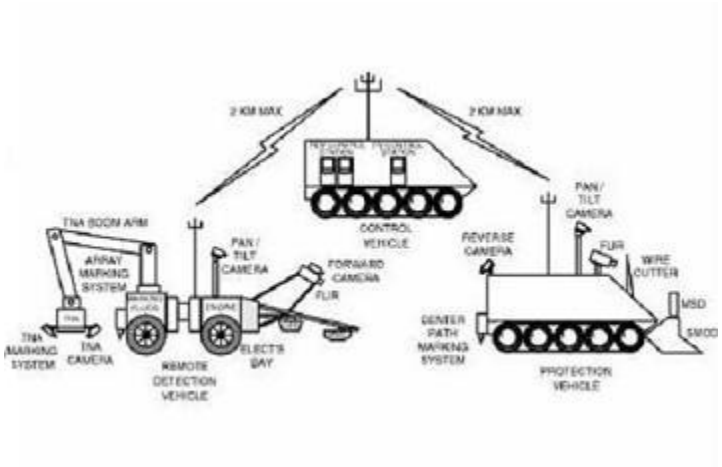


**Fig. 2.2.** Improved Landmine Detection System
from [33]

**Fig. 2.3.** DUNBLAD Apparatus
from [28]

### 2.15.4 Pulsed Elemental Analysis with Neutrons

The Pulsed Elemental Analysis with Neutrons (PELAN) system, created by Ancore (formerly Science Applications International Corporation) uses PFTNA by employing a pulsed deuterium-tritium neutron generator [10, 29, 34, 35]. It consists of two primary units: one composed of the power supply and neutron generator and the other of a BGO gamma ray detector and shielding [25, 34, 35]. The entire apparatus weighs approximately 40 kg [34, 35]. The neutron generator provides 10 microsecond pulses of 14-MeV neutrons [29, 34, 35]. The system is fully automated and is controlled with a palm or laptop computer [25, 34, 35]. The PELAN takes five minutes to analyze an object, is unaffected by temperature, and can operate up to six hours before its twelve volt battery must be recharged [10, 35]. The system compares the measurements to previous measurements to determine if an explosive is present [25]. The creators of the device see it as a confirmatory sensor [35].

### 2.15.5 Z® Backscatter Portal$^{TM}$ and Z® Backscatter Van$^{TM}$

Both the Z® Backscatter Portal and Z® Backscatter Van use transmission and backscatter x rays to create images of vehicles. The portal, shown in Figure 2.4 uses an array of 225 keV x-ray beams to create real-time images of vehicles traveling around six miles per hour. One


**Fig. 2.4.** Z Backscatter Portal
from http://www.as-e.com/products_solutions/cargo_vehicle_inspection.asp

scan produces one transmission image and three backscatter images. The transmission image displays the approximate density of the vehicle contents while the backscatter images, which are taken to the left, right, and above the vehicle, can be used to get an idea of the contents of the vehicle. The van, shown in Figure 2.5, uses a similar array of x-ray beams to create a single backscatter image. It is powered by an on-board generator so it can interrogate an object while the van is in motion. [36]

### 2.15.6 Other Projects

In addition to the projects described above, GE Security is creating a Quadrupole Resonance Confirmation Sensor (QRCS) that employs NQR [10]. The Nanosecond Neutron Analysis System (SENNA) uses API to find carbon to oxygen and oxygen to nitrogen ratios [10]. The Detection and Imaging of Anti-Personnel Landmines by Neutron Backscattering Techniques


**Fig. 2.5.** Z Backscatter Van
from http://www.as-e.com/products_solutions/cargo_vehicle_inspection.asp

(DIAMINE) system uses a $^{252}$Cf source to emit neutrons that backscatter with probability inversely proportional to the atomic number of the scattering element and undergo a residual energy loss that is also inversely proportional to the atomic number of the scattering element. The Hydrogen Density Anomaly Detection (HYDAD) system uses a AmBe or $^{252}$Cf source and one or more neutron detectors to detect neutrons moderated by hydrogen [10, 29]. The source-detector geometry is similar to that of DUNBLAD's but data processing and analysis are different [37].

# Chapter 3

# Theory of Signature-Based Radiation Scanning

The proposed method of explosives detection, introduced by Dunn et. al. [38], employs some of the concepts behind the methods detailed in Chapter 2. However, it differers from the techniques in that it seeks to detect if an explosive is present rather than measure the unknown object's content.

A photon and/or neutron beam is aimed at a target. Detectors, placed on the same side of the object as the photon and/or neutron beam record backscattered and generated responses. A figure-of-merit is used to calculate the statistical match between the template and the responses acquired. The neutron interrogation method is based on fast and thermal neutron backscattering and neutron-induced gamma rays from hydrogen, oxygen, carbon, and nitrogen. Hydrogen and nitrogen emit 2.223-MeV and 10.83-MeV prompt gamma rays, respectively, via neutron capture. Carbon emits a 4.43-MeV inelastic-scatter gamma ray; nitrogen emits 1.64-MeV, 2.31-MeV, and 5.11-MeV inelastic-scatter gamma rays; and oxygen emits a 6.128-MeV inelastic-scatter gamma ray. The response, $R_i$, at each energy $i$ is measured and compared to the template, $S_{li}$, which is the response of a known explosive in configuration $l$. $R_i$ and $S_{li}$ are used to calculate the figure-of-merit for a given configuration using Equation 3.1 below.

$$\varsigma_l = \sum_{i=1}^{N} \alpha_i \frac{(\beta R_i - S_{li})^2}{\beta^2 \sigma^2 (R_i) + \sigma^2 (S_{li})}, \tag{3.1}$$

where $N$ is the number of responses, $\beta$ scales the response to match the template, and $\alpha_i$ is

a normalized weight factor defined as

$$\alpha_i = \frac{\omega_i}{\sum_{i=1}^{N} \omega_i}, \tag{3.2}$$

where $\omega_i$ is the weight factor for the $i^{th}$ response, and $\sigma^2(R_i)$ is the variance of $R_i$ and $\sigma^2(S_{li})$ is the variance of $S_{li}$. Also, it can be shown that the standard deviation of the figure-of-merit can be expressed as

$$\sigma\left(\varsigma_l\right) = 2\left[\sum_{i=1}^{N} \alpha_i^2 \frac{\left(\beta R_i - S_{li}\right)^2}{\beta^2\sigma^2\left(R_i\right) + \sigma^2\left(S_{li}\right)}\right]^{\frac{1}{2}}, \tag{3.3}$$

A cutoff value $\varsigma_0$ will be established. If $\varsigma > \varsigma_0$ it is unlikely that the target contains an explosive; if $\varsigma \leq \varsigma_0$ the target is likely to contain an explosive. A database of templates reflecting several different common explosives in a variety of environments can be created.

Advantages of this method over those discussed in Chapter 2 include:

- a simplified process due to detecting the presence of an explosive rather than measuring the amount of explosive,
- does not require human interpretation of the response to determine if an explosive is present, and
- can be operated remotely, which increases the safety of the operator.

# Chapter 4

# Experiments and Results

## 4.1 Experimental Setup

The general setup for the experiments included the following equipment

- an aluminum box
- a Canberra high purity germanium (HPGe) detector model GC2019 (serial number 04057961) with cryostat model 7600 SI and preamplifier model 2002CSI
- the Kansas State University TRIGA Mark II Nuclear Research Reactor tangential beam port
- Canberra Genie 2000 3.1 computer software
- Canberra InSpector 2000 Model IN2K (serial number 05032284)

A photograph of the setup is shown in Figure 4.1. A typical spectrum produced by the Genie software is shown in Figure 4.2.

### 4.1.1 TRIGA Mark II Reactor

The Kansas State University TRIGA Mark II Nuclear Research Reactor tangential beam port is an aluminum tube six inches in diameter surrounded by an eight inch diameter cadmium-lined steel tube. The center of the beam tube is 2.75 inches below the reactor core centerline [39].

**Fig. 4.1.** Photograph of One Experimental Configuration

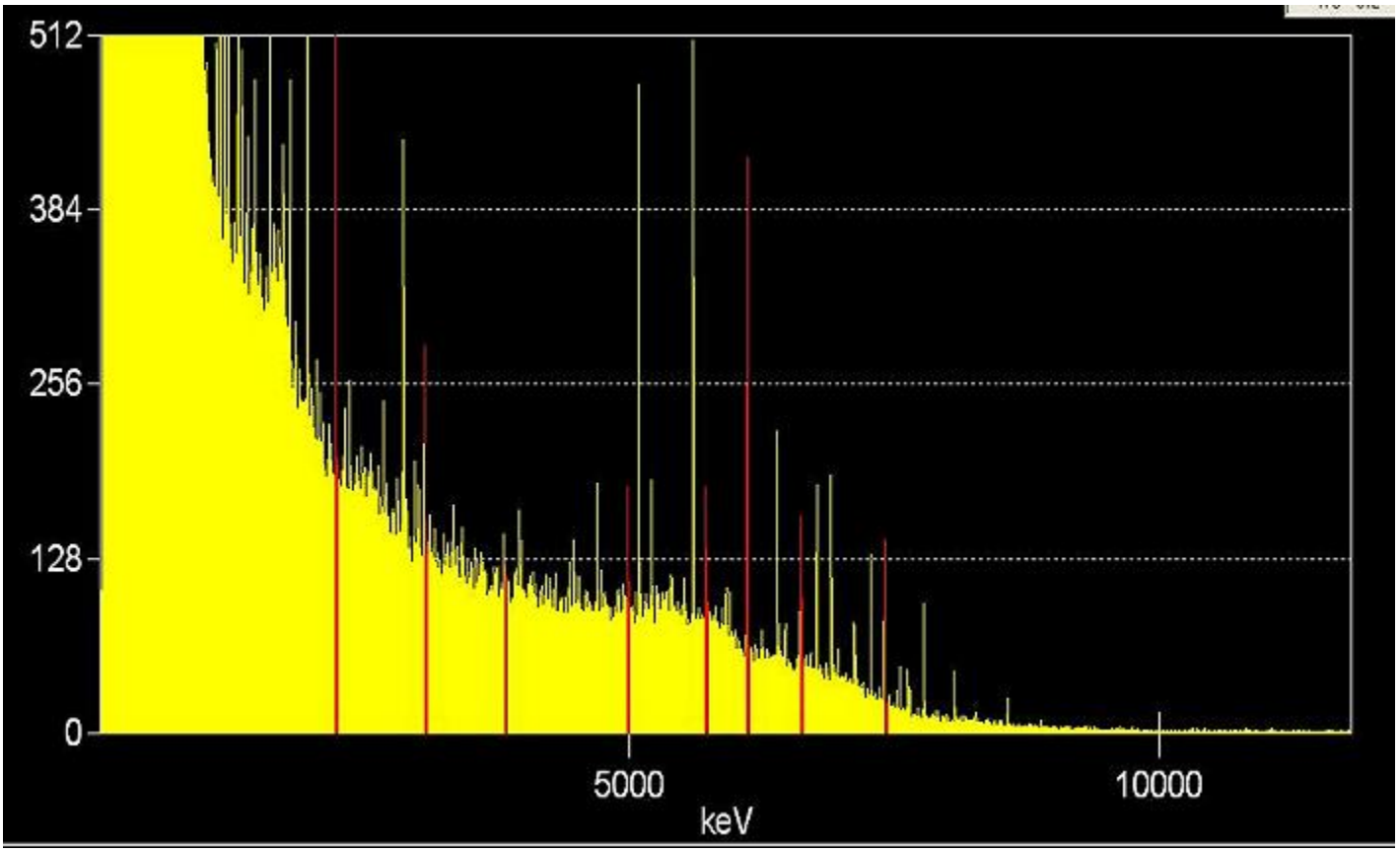


**Fig. 4.2.** Example Spectrum

### 4.1.2 Aluminum Box

The aluminum box was constructed of 0.0625 inch thick aluminum sheets. The box has dimensions of 3 feet by 3 feet by 3 feet When placed in front of the beam port it is raised 17.25 inches above the floor with a wooden pallet. Inside the box is a wood and aluminum platform that raises the sample 14.25 inches above the bottom of the box.

### 4.1.3 Samples Tested

The samples were selected based upon their representation of a number of chemicals and densities or based upon their common presence in vehicles. The samples tested on the various experiment dates include silica sand, water, calcium carbonate (chalk), rubber (mulched), aluminum, fertilizer, antifreeze, windshield washer fluid, black car paint, soybeans, and polyethylene. Three types of fertilizer were used to simulate explosives: the two listed in Table 4.1 and a 50-50 mixture of the two.

**Table 4.1.** Types of Fertilizer

| Manufacturer | Brand | Name | % $^{14}$N |
|---|---|---|---|
| Free Flow | Green Thumb | Premium Lawn Fertilizer 30-3-3 | 30 |
| Scotts | Lawn Pro | Super Turf Builder w/ Halts Crabgrass Preventer 36-3-4 | 36 |

## 4.2 Experiments

### 4.2.1 October 25, 2005

The experiment performed October 25, 2005 used a 20% efficient HPGe detector, a Bicron model 802-3x3 three by three NaI detector (serial number 08067856) connected to a Canberra Unispec (serial number 22060239), and a $^{3}$He detector with the NIM components listed in Table 4.2. The experiment configuration is shown in Figure 4.3. A two gallon plastic can containing disel fuel was placed inside the aluminum box as well as a one gallon paint can filled with granulated sugar. The samples were contained in 10 gallon drums. The neutron

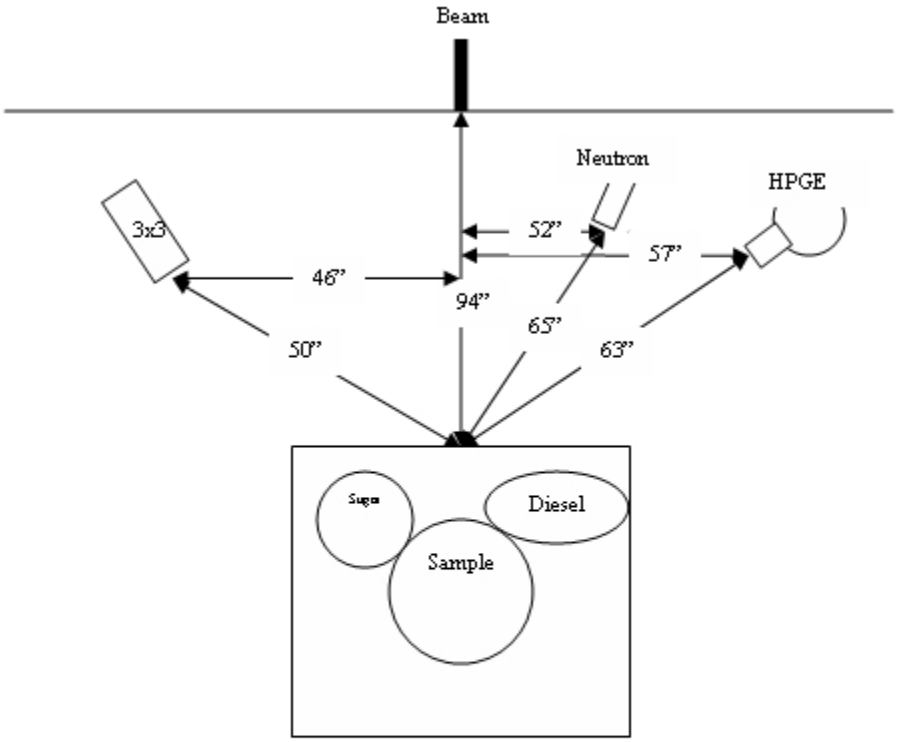


**Fig. 4.3.** October 25, 2005 Experiment Configuration

detector was set to a high voltage of 800 V, a coarse gain of 8, and a fine gain of 0. The lower and upper level discriminators were set at 24 and 100, respectively. The reactor operated at 240 kW and data were taken for forty minutes of live time, twenty minutes of which a cadmium sheet was placed in front of the neutron detector.

The data acquired from the neutron detector are shown in Table 4.3. The counts and standard deviation obtained from the Genie software outputs for the pertinent energies are shown in Table 4.4. The pertinent NaI data from the Genie software output are shown in Table 4.5. The figure-of-merit for each sample was calculated using the thirty percent fertilizer as the template. These values are shown in Table 4.6.

The results for all these inert samples are significantly greater than zero indicating that

**Table 4.2.** NIM Components

| Component | Make | Model | Serial Number |
|---|---|---|---|
| NIM Bin | Tennelec | TB3 | 6079 |
| NIM Power Supply | Tennelec | TC911-6 | 251 |
| Pre-Amplifier | Canberra | 2006 | 07041903 |
| High Voltage Power Supply | Bertran | 353 | 800 |
| Amplifier | Canberra | 2012 | 681933 |
| Single Channel Analyzer | Ortec | 406A | 2604 |
| Scaler | Canberra | 1773 | 481210 |
| Counter/Timer | Tennelec | TC545A | 200 |

**Table 4.3.** Neutron Data - October 25, 2005

| Sample | $R_i$ without Cd | $\sigma(R_i)$ | $R_i$ with Cd | $\sigma(R_i)$ |
|---|---|---|---|---|
| Air | 2193 | 47 | 2048 | 45 |
| Aluminum | 2736 | 52 | 2308 | 48 |
| Fertilizer 30 | 3393 | 58 | 2813 | 53 |
| Sand | 3374 | 58 | 2624 | 51 |
| Water | 3939 | 63 | 3245 | 57 |

they are not explosives. From the results, it can be concluded that inert samples tend to give large figure-of-merit values, hopefully allowing differentiation from explosives.

### 4.2.2 April 20, 2006

The experiment performed April 20, 2006 used the HPGe and Bicron model 802-3x3 three by three NaI detectors used on October 25, 2005 connected to the same Canberra Unispec. The aluminum box was placed 94 inches from the beam collimator with a car windshield in from of it. The HPGe detector was 57 inches from the center of the beam and the NaI detector was 46 inches from the center of the beam on the side of the beam opposite the HPGe detector. The samples were placed in ten gallon drums. The samples tested were

**Table 4.4.** HPGe Data - October 25,2005

| $R_i$ (i in MeV) | Air | Aluminum | Fertilizer 30 | Sand | Water |
|---|---|---|---|---|---|
| $R_{0.871}$ | 15825 | 15713 | 19084 | 15233 | 15161 |
| $\sigma(R_{0.871})$ | 509 | 2901 | 2777 | 2991 | 3543 |
| $R_{1.262}$ | 507 | 857 | 1183 | 0 | 1734 |
| $\sigma(R_{1.262})$ | 44 | 74 | 90 | 0 | 160 |
| $R_{1.64}$ | 437 | 951 | 0 | 366 | 0 |
| $\sigma(R_{1.64})$ | 232 | 237 | 0 | 277 | 345 |
| $R_{1.885}$ | 1555 | 0 | 0 | 55 | 404 |
| $\sigma(R_{1.885})$ | 504 | 0 | 300 | 32 | 292 |
| $R_{2.223}$ | 8968 | 15340 | 22156 | 14866 | 76398 |
| $\sigma(R_{2.223})$ | 475 | 1390 | 239 | 334 | 771 |
| $R_{2.31}$ | 0 | 103 | 716 | 270 | 0 |
| $\sigma(R_{2.31})$ | 0 | 207 | 101 | 226 | 0 |
| $R_{4.43}$ | 1436 | 1024 | 1132 | 2265 | 1152 |
| $\sigma(R_{4.43})$ | 307 | 79 | 248 | 271 | 90 |
| $R_{4.945}$ | 767 | 1236 | 14 | 2730 | 1267 |
| $\sigma(R_{4.945})$ | 52 | 64 | 446 | 76 | 66 |
| $R_{5.11}$ | 0 | 0 | 0 | 0 | 0 |
| $\sigma(R_{5.11})$ | 0 | 169 | 0 | 0 | 0 |

rubber, aluminum, silica sand, fertilizer 30%, polyethylene, and an empty barrel (air). Each sample was analyzed for 1200 seconds live time. The reactor operated at 240 kW.

The counts and standard deviation obtained from the Genie software outputs for the pertinent energies are shown in Table 4.7. The pertinent NaI data from the Genie software output are shown in Table 4.8. The figures-of-merit for the neutron induced gamma ray data from the HPGe with the fertilizer 30% serving as the template are listed in Table 4.9.

The data obtained from the NaI detector were not specific enough for analysis and therefore were not used in calculating the figures-of-merit. A high number of counts only occur at a few energies, most of which are the result of backscattering. These data are not as useful

**Table 4.5.** NaI(Tl) Data - October 25, 2005

| $R_i$ (i in MeV) | Air | Al | Fert30 | Sand | Water |
|---|---|---|---|---|---|
| $R_{0.871}$ | 0 | 28601 | 0 | 0 | 0 |
| $\sigma(R_{0.871})$ | 0 | 2613 | 0 | 0 | |
| $R_{1.262}$ | 0 | 0 | 0 | 15811 | 0 |
| $\sigma(R_{1.262})$ | 0 | 0 | 0 | 1645 | 0 |
| $R_{1.64}$ | 0 | 0 | 0 | 18377 | 0 |
| $\sigma(R_{1.64})$ | 0 | 0 | 0 | 1161 | 0 |
| $R_{1.885}$ | 0 | 0 | 0 | 37760 | 0 |
| $\sigma(R_{1.885})$ | 0 | 0 | 0 | 1131 | |

**Table 4.6.** October 25, 2005 Figures-of-Merit

| Sample | $\varsigma$ | $\sigma(\varsigma)$ |
|---|---|---|
| Air | 276.420 | 5.766 |
| Aluminum | 45.903 | 3.681 |
| Sand | 136.491 | 4.834 |
| Water | 1163.937 | 8.260 |

as the HPGe data, so use of the NaI detector for detection of neutron induced gamma rays was discontinued in all subsequent experiments.

The figures-of-merit for all the inert samples were again significantly greater than zero indicating that they are not explosives. From the results, it can be concluded that inert samples tend to give large figure-of-merit values differentiating them from the fertilizer.

### 4.2.3 May 7, 2007

The experiment performed May 7, 2007 used the HPGe detector as well as two Scionix Holland type 25B3/LM-E1-L-X europium doped lithium iodide (LiI(Eu)) neutron detectors (serial numbers SAV804 and SAV805) each with a Spectrum Techniques Spectech Model ST360 counters (serial numbers 1219 and 1221). The neutron detector crystals are 25 mil-

**Table 4.7.** HPGe Data - April 20, 2006

| $R_i$ (i in MeV) | Air | Al | Fert30 | Poly | Rubber | Sand |
|---|---|---|---|---|---|---|
| $R_{0.871}$ | 3487 | 4989 | 5955 | 6951 | 6891 | 6144 |
| $\sigma(R_{0.871})$ | 234 | 111 | 171 | 166 | 187 | 191 |
| $R_{1.262}$ | 0 | 428 | 353 | 610 | 698 | 479 |
| $\sigma(R_{1.262})$ | 0 | 44 | 53 | 68 | 61 | 55 |
| $R_{1.64}$ | 0 | 0 | 154 | 0 | 0 | 0 |
| $\sigma(R_{1.64})$ | 0 | 0 | 77 | 0 | 0 | 0 |
| $R_{1.885}$ | 0 | 0 | 299 | 0 | 0 | 0 |
| $\sigma(R_{1.885})$ | 0 | 0 | 80 | 0 | 0 | 0 |
| $R_{2.223}$ | 3760 | 5543 | 12356 | 33726 | 22472 | 6361 |
| $\sigma(R_{2.223})$ | 132 | 123 | 159 | 221 | 191 | 129 |
| $R_{2.31}$ | 0 | 138 | 0 | 0 | 0 | 0 |
| $\sigma(R_{2.31})$ | 0 | 57 | 0 | 0 | 0 | 0 |

limeters by 3 millimeters and are mounted in an aluminum housing with a Mu-metal shield and a built in voltage divider of 6 megaohms. Each of the Spectech counters was set to a high voltage of 380 V. The aluminum box was placed 88 inches from the beam collimator with a car windshield in front of it. The HPGe detector was 54 inches in front of and 63.75 inches from the center of the beam. Both neutron detectors were 50 inches in front of and 79.2 inches from the center of the beam. The bare neutron detector was 33.5 inches above the floor and the cadmium covered detector was 30 inches above the floor. The samples were placed in 5 gallon buckets. The buckets are 13 inches tall with an inner diameter of 11.5 inches and an outer diameter of 11.875 inches. The samples tested were rubber, aluminum, silica sand, water, calcium carbonate, fertilizer 30-3-3, fertilizer 36-3-4, fertilizer mix, polyethylene, and an empty barrel (air). Each sample was analyzed for 2000 seconds. The reactor operated at 120 kW.

The data acquired from the neutron detector are shown in Table 4.10. The counts and standard deviation obtained from the Genie software outputs for the pertinent energies are

**Table 4.8.** NaI(Tl) Data - April 20, 2006

| $R_i$ (i in MeV) | Air | Al | Fert30 | Poly | Rubber | Sand |
|---|---|---|---|---|---|---|
| $R_{0.871}$ | 1089482 | 55359 | 0 | 0 | 83177 | 0 |
| $\sigma(R_{0.871})$ | 114 | 6834 | 0 | 0 | 6883 | 0 |
| $R_{1.262}$ | 1077451 | 0 | 0 | 38709 | 0 | 0 |
| $\sigma(R_{1.262})$ | 110 | 0 | 0 | 1942 | 0 | 0 |
| $R_{1.64}$ | 0 | 0 | 0 | 0 | 0 | 77114 |
| $\sigma(R_{1.64})$ | 0 | 0 | 0 | 0 | 0 | 5931 |
| $R_{1.885}$ | 0 | 160548 | 34660 | 32717 | 20103 | 37457 |
| $\sigma(R_{1.885})$ | 0 | 8188 | 6893 | 3143 | 2899 | 8418 |
| $R_{2.223}$ | 0 | 186233 | 81153 | 372937 | 297710 | 192045 |
| $\sigma(R_{2.223})$ | 0 | 7163 | 7819 | 22822 | 15624 | 8196 |

**Table 4.9.** April 20, 2006 Figures-of-Merit

| Sample | $\varsigma$ | $\sigma(\varsigma)$ |
|---|---|---|
| Air | 373.023 | 6.215 |
| Aluminum | 239.224 | 5.562 |
| Polyethylene | 1241.095 | 8.394 |
| Rubber | 341.348 | 6.079 |
| Sand | 175.708 | 5.149 |

shown in Table 4.11. The figures-of-merit for the neutron and neuton-induced gamma ray data with the fertilizer mix serving as the template are listed in Table 4.12.

The results of this experiment show significant differences between the simulated explosives and the inert materials. The figures-of-merit for the fertilizers and both less than 10 while all the inert materials have figures-of-merit greater than 75. A good cutoff value for this experiment would be about 50. It can now be concluded that the template-matching technique can be used to detect explosives.

**Table 4.10.** Neutron Data - May 7, 2007

| Sample | $R_i$ without Cd | $\sigma(R_i)$ | $R_i$ with Cd | $\sigma(R_i)$ |
|---|---|---|---|---|
| Air | 299308 | 547 | 37918 | 195 |
| Aluminum | 341670 | 585 | 50345 | 224 |
| Chalk | 357442 | 598 | 49484 | 222 |
| Fertilizer 30 | 333335 | 577 | 42262 | 206 |
| Fertilizer 36 | 341938 | 585 | 43856 | 209 |
| Fertilizer Mix | 337237 | 581 | 42191 | 205 |
| Polyethylene | 354355 | 595 | 42143 | 205 |
| Rubber | 397901 | 631 | 51969 | 228 |
| Sand | 378537 | 615 | 53570 | 231 |
| Water | 313774 | 560 | 38906 | 197 |

### 4.2.4 August 6, 2007

The experiment performed August 6, 2007 used the HPGe detector as well as the two Scionix Holland LiI(Eu) neutron detectors each with a Spectrum Techniques Spectech Model ST360 counters set to a high voltage of 380 V. The aluminum box was place 93 inches from the beam collimator with a car windshield in front of the box. The HPGe detector was 57 inches in front of and 54 inches from the center of the beam. Both neutron detectors were 50 inches in front of and 79.2 inches from the center of the beam. The bare neutron detector was 46.5 inches above the floor and the cadmium covered detector was 44.5 inches above the floor. The samples were placed in one gallon paint cans. Samples tested were rubber, aluminum, silica sand, water, calcium carbonate, fertilizer 30-3-3, fertilizer 36-3-4, fertilizer mix, polyethylene, and soybeans. Each sample was analyzed for 1000 seconds. The reactor operated at 185 kW.

The data acquired from the neutron detector are shown in Table 4.13 and the data from the HPGe detector are shown in Table 4.14 with the number of counts and standard deviation obtained from the Genie software outputs. The figures-of-merit for the neutron and neutron-induced gamma ray data with the fertilizer mix serving as the template are

**Table 4.11.** HPGe Data - May 7 , 2007

| $R_i$ (i in MeV) | Air | Al | Chalk | Fert30 | Fert36 | FertMix | Poly | Rubber | Sand | Water |
|---|---|---|---|---|---|---|---|---|---|---|
| $R_{0.871}$ | 6631 | 0 | 5612 | 10120 | 5148 | 6187 | 4698 | 2338 | 5010 | 0 |
| $\sigma(R_{0.871})$ | 1082 | 0 | 1110 | 37 | 454 | 1183 | 1229 | 37 | 1160 | 0 |
| $R_{1.262}$ | 185 | 0 | 0 | 0 | 0 | 0 | 504 | 0 | 0 | 582 |
| $\sigma(R_{1.262})$ | 36 | 0 | 0 | 0 | 0 | 0 | 31 | 0 | 0 | 49 |
| $R_{1.64}$ | 0 | 0 | 0 | 0 | 0 | 0 | 0 | 0 | 33 | 0 |
| $\sigma(R_{1.64})$ | 0 | 0 | 0 | 0 | 0 | 0 | 0 | 0 | 16 | 0 |
| $R_{1.885}$ | 0 | 0 | 0 | 0 | 0 | 0 | 0 | 0 | 0 | 0 |
| $\sigma(R_{1.885})$ | 0 | 0 | 0 | 0 | 0 | 0 | 0 | 0 | 0 | 0 |
| $R_{2.223}$ | 7627 | 5514 | 5514 | 7428 | 7882 | 7713 | 15299 | 10650 | 5616 | 16950 |
| $\sigma(R_{2.223})$ | 240 | 134 | 87 | 149 | 168 | 153 | 187 | 258 | 139 | 178 |
| $R_{2.31}$ | 0 | 0 | 0 | 225 | 0 | 0 | 0 | 0 | 0 | 0 |
| $\sigma(R_{2.31})$ | 0 | 0 | 0 | 115 | 0 | 0 | 0 | 0 | 0 | 0 |
| $R_{4.43}$ | 486 | 475 | 728 | 600 | 646 | 396 | 784 | 41 | 989 | 404 |
| $\sigma(R_{4.43})$ | 52 | 41 | 97 | 56 | 121 | 100 | 128 | 193 | 122 | 99 |
| $R_{4.945}$ | 146 | 468 | 532 | 268 | 842 | 291 | 532 | 553 | 770 | 441 |
| $\sigma(R_{4.945})$ | 139 | 35 | 38 | 139 | 197 | 194 | 39 | 42 | 47 | 36 |
| $R_{5.11}$ | 0 | 0 | 69 | 255 | 209 | 205 | 46 | 0 | 0 | 0 |
| $\sigma(R_{5.11})$ | 0 | 0 | 107 | 102 | 92 | 99 | 106 | 0 | 0 | 0 |
| $R_{6.128}$ | 140 | 0 | 0 | 779 | 0 | 301 | 210 | 226 | 180 | 0 |
| $\sigma(R_{6.128})$ | 82 | 0 | 0 | 128 | 0 | 94 | 82 | 92 | 91 | 0 |

**Table 4.12.** May 7, 2006 Figures-of-Merit

| Sample | $\varsigma$ | $\sigma(\varsigma)$ |
|---|---|---|
| Air | 279.483 | 5.782 |
| Aluminum | 99.990 | 4.472 |
| Chalk | 148.225 | 4.935 |
| Fertilizer 30% | 4.747 | 2.087 |
| Fertilizer 36% | 8.065 | 2.383 |
| Polyethylene | 157.628 | 5.011 |
| Rubber | 681.580 | 13.054 |
| Sand | 430.251 | 7.226 |
| Water | 300.102 | 5.886 |

listed in Table 4.15.

The results do not display as significant differences between the simulated explosives and the inert materials as in the May 7, 2007 experiments. This can be attributed to the smaller sample size. However, the explosives stimulants still have values close to zero and a cut-off values of about 15 would differentiate inert from explosive-like samples.

### 4.2.5 August 14, 2007

The experiment performed August 14, 2007 used the HPGe detector as well as the two Scionix Holland LiI(Eu) neutron detectors each with a Spectrum Techniques Spectech Model ST360 counters set to a high voltage of 380 V. The aluminum box was place 93 inches from the beam collimator with a car windshield in front of the box. The HPGe detector was 57 inches in front of and 54 inches from the center of the beam. Both neutron detectors were 50 inches in front of and 79.2 inches from the center of the beam. The bare neutron detector was 46.5 inches above the floor and the cadmium covered detector was 44.5 inches above the floor. The samples were placed in one quart paint cans. Samples tested were rubber, aluminum, silica sand, water, calcium carbonate, fertilizer 30-3-3, fertilizer 36-3-4, fertilizer mix, polyethylene, antifreeze, black car paint, windshield washer fluid, and an empty barrel

**Table 4.13.** Neutron Data - August 6, 2007

| Sample | $R_i$ without Cd | $\sigma(R_i)$ | $R_i$ with Cd | $\sigma(R_i)$ |
|---|---|---|---|---|
| Aluminum | 182523 | 427 | 32752 | 181 |
| Chalk | 234920 | 485 | 41781 | 204 |
| Fertilizer 30 | 237882 | 488 | 41924 | 205 |
| Fertilizer 36 | 238535 | 488 | 41008 | 203 |
| Fertilizer Mix | 236768 | 487 | 41121 | 203 |
| Polyethylene | 240957 | 491 | 39710 | 199 |
| Rubber | 272481 | 522 | 44920 | 212 |
| Sand | 252112 | 502 | 44082 | 210 |
| Soybeans | 256266 | 506 | 42573 | 206 |
| Water | 247874 | 498 | 40083 | 200 |

(air). Each sample was analyzed for 1000 seconds. The reactor operated at 175 kW.

The data acquired from the neutron detector are shown in Table 4.16 and the data from the HPGe detector are shown in Table 4.17 with the number of counts and standard deviation obtained from the Genie software outputs. The figures-of-merit for the neutron and neutron-induced gamma ray data with the fertilizer mix serving as the template are listed in Table 4.18.

The results of this experiment do not conclusively distinguish the inert materials from the simulated explosives. However, it is thought that the sample placement in relation to the detector may be off so the detector cannot "see" the sample.

### 4.2.6 October 3, 2007

This experiment is a rerun of the August 14, 2007 experiment. However, the bottom of the HPGe detector's dewar is raised 4.5 inches above the floor. The detector center is 31.75 inches above the floor, 57 inches from the beam port center , 52.75 inches from the reactor and 39.75 inches from the box front. The cadmium covered neutron detector is 33.5 inches above the floor, 64 inches from the reactor, 68 inches from the beam port centerline, and

25.5 inches from the box front.

The data acquired from the neutron detector are shown in Table 4.19 and the data from the HPGe detector are shown in Table 4.20 with the number of counts and standard deviation obtained from the Genie software outputs. The figures-of-merit for the neutron and neutron-induced gamma ray data with the fertilizer 30 serving as the template are listed in Table 4.21. The figures-of-merit for the neutron and neutron-induced gamma ray data with the fertilizer 36 serving as the template are listed in Table 4.22. The figures-of-merit for the neutron and neutron-induced gamma ray data with the fertilizer mix serving as the template are listed in Table 4.23.

As shown in the above tables, the system is again generally able to distinguish between explosives and non-explosives. These results can lead to the conclusion that the template matching technique works for samples of quantities as small as one quart. The few instances in which an inert sample's figure-of-merit is less than the figure-of-merit if the simulated explosives means that a few false positives might occur with very small sample sizes. It may be that this can be remedied by calculating weight factors for each of the response energies for the figure-of-merit equation.

**Table 4.14.** HPGe Data - August 6, 2007

| $R_i$ (i in MeV) | Al | Chalk | Fert30 | Fert36 | FertMix | Poly | Rubber | Sand | Soybeans | Water |
|---|---|---|---|---|---|---|---|---|---|---|
| $R_{0.871}$ | 2446 | 2028 | 4923 | 2372 | 6038 | 1883 | 3023 | 2035 | 3472 | 3143 |
| $\sigma(R_{0.871})$ | 619 | 632 | 122 | 639 | 14 | 701 | 37 | 40 | 79 | 714 |
| $R_{1.262}$ | 0 | 0 | 356 | 138 | 0 | 131 | 0 | 364 | 281 | 0 |
| $\sigma(R_{1.262})$ | 0 | 0 | 127 | 112 | 0 | 129 | 0 | 71 | 118 | 0 |
| $R_{1.64}$ | 581 | 801 | 482 | 526 | 534 | 501 | 384 | 0 | 545 | 215 |
| $\sigma(R_{1.64})$ | 197 | 157 | 52 | 195 | 266 | 120 | 115 | 215 | 116 | 155 |
| $R_{1.885}$ | 2984 | 1996 | 1933 | 1816 | 1994 | 1696 | 2053 | 1831 | 2572 | 2013 |
| $\sigma(R_{1.885})$ | 146 | 142 | 157 | 139 | 142 | 128 | 133 | 110 | 145 | 130 |
| $R_{2.223}$ | 3533 | 3949 | 6797 | 7411 | 7005 | 12401 | 8130 | 4514 | 10132 | 13504 |
| $\sigma(R_{2.223})$ | 123 | 152 | 133 | 161 | 134 | 179 | 139 | 123 | 141 | 158 |
| $R_{2.31}$ | 0 | 0 | 0 | 0 | 0 | 0 | 0 | 0 | 0 | 0 |
| $\sigma(R_{2.31})$ | 0 | 0 | 0 | 0 | 0 | 0 | 0 | 0 | 0 | 0 |
| $R_{4.43}$ | 144 | 0 | 230 | 0 | 0 | 0 | 308 | 393 | 223 | 560 |
| $\sigma(R_{4.43})$ | 77 | 0 | 95 | 0 | 0 | 0 | 82 | 86 | 87 | 106 |
| $R_{4.945}$ | 408 | 134 | 204 | 51 | 254 | 278 | 445 | 471 | 309 | 329 |
| $\sigma(R_{4.945})$ | 43 | 116 | 30 | 99 | 32 | 34 | 39 | 38 | 32 | 88 |
| $R_{5.11}$ | 0 | 0 | 366 | 192 | 24 | 41 | 133 | 85 | 139 | 0 |
| $\sigma(R_{5.11})$ | 0 | 0 | 88 | 71 | 85 | 71 | 77 | 73 | 74 | 0 |
| $R_{6.128}$ | 0 | 0 | 483 | 0 | 321 | 0 | 0 | 0 | 0 | 0 |
| $\sigma(R_{6.128})$ | 0 | 0 | 83 | 0 | 81 | 0 | 0 | 0 | 0 | 0 |

**Table 4.15.** August 6, 2007 Figures-of-Merit

| Sample | $\varsigma$ | $\sigma(\varsigma)$ |
|---|---|---|
| Aluminum | 932.593 | 7.815 |
| Chalk | 31.333 | 3.346 |
| Fertilizer 30% | 12.996 | 2.685 |
| Fertilizer 36% | 5.756 | 2.191 |
| Polyethylene | 75.842 | 4.173 |
| Rubber | 958.815 | 7.869 |
| Sand | 1084.831 | 8.116 |
| Soybeans | 233.357 | 5.527 |
| Water | 144.192 | 4.901 |

**Table 4.16.** Neutron Data - August 14, 2007

| Sample | $R_i$ without Cd | $\sigma(R_i)$ | $R_i$ with Cd | $\sigma(R_i)$ |
|---|---|---|---|---|
| Air | 49277 | 222 | 11492 | 107 |
| Aluminum | 77685 | 279 | 17069 | 131 |
| Antifreeze | 141169 | 376 | 25723 | 160 |
| Chalk | 127753 | 357 | 25415 | 159 |
| Fertilizer 30 | 155121 | 394 | 30202 | 174 |
| Fertilizer 36 | 140638 | 375 | 26977 | 164 |
| Fertilizer Mix | 172930 | 416 | 32327 | 180 |
| Paint | 134319 | 366 | 27197 | 165 |
| Polyethylene | 122400 | 350 | 22466 | 150 |
| Rubber | 150080 | 387 | 27655 | 166 |
| Sand | 119422 | 346 | 23859 | 154 |
| Washer Fluid | 174240 | 417 | 30305 | 174 |
| Water | 162772 | 403 | 28139 | 168 |

**Table 4.17.** HPGe Data - August 14, 2007

| $R_i$ (i in MeV) | Air | Al | Antifrz | Paint | Chalk | Fert30 | Fert36 | FertMix | Poly | Rubber | Sand | WshrFl | Water |
|---|---|---|---|---|---|---|---|---|---|---|---|---|---|
| $R_{0.871}$ | 887 | 1496 | 2260 | 1568 | 2926 | 3373 | 3374 | 2471 | 577 | 3264 | 1813 | 1470 | 3907 |
| $\sigma(R_{0.871})$ | 48 | 71 | 461 | 235 | 31 | 104 | 45 | 126 | 11 | 33 | 246 | 35 | 35 |
| $R_{1.262}$ | 0 | 0 | 200 | 0 | 0 | 0 | 191 | 238 | 0 | 367 | 0 | 308 | 213 |
| $\sigma(R_{1.262})$ | 0 | 0 | 98 | 0 | 0 | 0 | 96 | 109 | 0 | 102 | 0 | 110 | 127 |
| $R_{1.64}$ | 73 | 144 | 319 | 138 | 69 | 87 | 408 | 179 | 343 | 563 | 438 | 55 | 212 |
| $\sigma(R_{1.64})$ | 95 | 93 | 120 | 69 | 137 | 121 | 121 | 188 | 119 | 152 | 111 | 194 | 112 |
| $R_{1.885}$ | 681 | 2042 | 1584 | 1554 | 1387 | 1652 | 1501 | 1845 | 1257 | 1650 | 1389 | 1863 | 1631 |
| $\sigma(R_{1.885})$ | 62 | 88 | 119 | 142 | 93 | 105 | 122 | 136 | 89 | 108 | 84 | 113 | 107 |
| $R_{2.223}$ | 606 | 931 | 6228 | 4614 | 1568 | 4085 | 3586 | 4266 | 6719 | 3670 | 1476 | 9250 | 8346 |
| $\sigma(R_{2.223})$ | 54 | 67 | 111 | 110 | 88 | 130 | 101 | 103 | 115 | 109 | 101 | 129 | 125 |
| $R_{2.31}$ | 0 | 0 | 0 | 0 | 0 | 0 | 0 | 0 | 0 | 0 | 0 | 0 | 0 |
| $\sigma(R_{2.31})$ | 0 | 0 | 0 | 0 | 0 | 0 | 0 | 0 | 0 | 0 | 0 | 0 | 0 |
| $R_{4.43}$ | 0 | 0 | 0 | 0 | 33 | 0 | 0 | 0 | 0 | 0 | 170 | 0 | 176 |
| $\sigma(R_{4.43})$ | 0 | 0 | 0 | 0 | 65 | 0 | 0 | 0 | 0 | 0 | 60 | 0 | 62 |
| $R_{4.945}$ | 0 | 160 | 86 | 606 | 56 | 19 | 0 | 229 | 127 | 172 | 167 | 44 | 126 |
| $\sigma(R_{4.945})$ | 0 | 49 | 76 | 76 | 51 | 89 | 0 | 25 | 50 | 60 | 21 | 63 | 23 |
| $R_{5.11}$ | 0 | 0 | 0 | 0 | 0 | 312 | 0 | 0 | 0 | 0 | 0 | 0 | 0 |
| $\sigma(R_{5.11})$ | 0 | 0 | 0 | 0 | 0 | 67 | 0 | 0 | 0 | 0 | 0 | 0 | 0 |
| $R_{6.128}$ | 0 | 0 | 0 | 982 | 0 | 358 | 0 | 234 | 0 | 0 | 0 | 0 | 0 |
| $\sigma(R_{6.128})$ | 0 | 0 | 0 | 87 | 0 | 69 | 0 | 73 | 0 | 0 | 0 | 0 | 0 |

**Table 4.18.** August 14, 2007 Figures-of-Merit

| Sample | $\varsigma$ | $\sigma(\varsigma)$ |
|---|---|---|
| Air | 6662.224 | 12.777 |
| Aluminum | 3470.337 | 10.854 |
| Antifreeze | 344.497 | 6.093 |
| Chalk | 670.935 | 7.198 |
| Fertilizer 30% | 91.905 | 4.379 |
| Fertilizer 36% | 330.283 | 6.029 |
| Paint | 445.270 | 6.496 |
| Polyethylene | 7469.561 | 13.147 |
| Rubber | 169.965 | 5.106 |
| Sand | 955.234 | 7.862 |
| Washer Fluid | 87.351 | 4.323 |
| Water | 135.422 | 4.824 |

**Table 4.19.** Neutron Data - October 3, 2007

| Sample | $R_i$ without Cd | $\sigma(R_i)$ | $R_i$ with Cd | $\sigma(R_i)$ |
|---|---|---|---|---|
| Background | 92499 | 304 | 20605 | 144 |
| Aluminum | 167923 | 410 | 34638 | 186 |
| Antifreeze | 246934 | 497 | 42326 | 206 |
| Black Car Paint | 250810 | 501 | 47148 | 217 |
| Chalk | 198578 | 446 | 38079 | 195 |
| Fertilizer 30% | 248896 | 499 | 45208 | 213 |
| Fertilizer 36% | 268469 | 518 | 47098 | 217 |
| Fertilizer Mix | 244523 | 494 | 44390 | 211 |
| Polyethylene | 255726 | 506 | 39318 | 198 |
| Rubber | 266663 | 516 | 45219 | 213 |
| Sand | 208050 | 456 | 40236 | 201 |
| Water | 266440 | 516 | 40465 | 201 |
| Washer Fluid | 294930 | 543 | 48515 | 220 |

**Table 4.20.** HPGe Data - October 3, 2007

| $R_i$ (i in MeV) | Air | Al | Antifrz | Paint | Chalk | Fert30 | Fert36 | FertMix | Poly | Rubber | Sand | Washer Fld | Water |
|---|---|---|---|---|---|---|---|---|---|---|---|---|---|
| $R_{0.871}$ | 538 | 1537 | 4715 | 2824 | 1991 | 2121 | 4587 | 4437 | 2133 | 4637 | 1369 | 3175 | 2445 |
| $\sigma(R_{0.871})$ | 45 | 56 | 120 | 94 | 18 | 145 | 41 | 41 | 638 | 38 | 589 | 663 | 689 |
| $R_{1.262}$ | 154 | 209 | 120 | 0 | 251 | 144 | 339 | 0 | 0 | 0 | 0 | 343 | 129 |
| $\sigma(R_{1.262})$ | 66 | 85 | 109 | 0 | 91 | 90 | 102 | 0 | 0 | 0 | 0 | 132 | 102 |
| $R_{1.64}$ | 426 | 472 | 458 | 785 | 364 | 592 | 436 | 297 | 423 | 509 | 361 | 534 | 538 |
| $\sigma(R_{1.64})$ | 78 | 115 | 97 | 176 | 79 | 188 | 139 | 110 | 117 | 130 | 89 | 126 | 96 |
| $R_{1.885}$ | 786 | 2789 | 1639 | 1192 | 1221 | 1397 | 1939 | 1472 | 1618 | 1527 | 1428 | 1342 | 1545 |
| $\sigma(R_{1.885})$ | 77 | 96 | 105 | 113 | 81 | 94 | 104 | 113 | 97 | 108 | 83 | 104 | 110 |
| $R_{2.223}$ | 810 | 1301 | 6207 | 4736 | 1328 | 3471 | 3986 | 3654 | 7820 | 3666 | 1566 | 8904 | 7917 |
| $\sigma(R_{2.223})$ | 69 | 82 | 112 | 110 | 82 | 97 | 130 | 112 | 124 | 102 | 80 | 141 | 132 |
| $R_{2.31}$ | 0 | 0 | 0 | 0 | 0 | 0 | 0 | 0 | 0 | 0 | 0 | 0 | 0 |
| $\sigma(R_{2.31})$ | 0 | 0 | 0 | 0 | 0 | 0 | 0 | 0 | 0 | 0 | 0 | 0 | 0 |
| $R_{4.43}$ | 0 | 0 | 0 | 0 | 228 | 0 | 0 | 0 | 0 | 0 | 269 | 0 | 0 |
| $\sigma(R_{4.43})$ | 0 | 0 | 0 | 0 | 61 | 0 | 0 | 0 | 0 | 0 | 76 | 0 | 0 |
| $R_{4.945}$ | 122 | 313 | 179 | 0 | 221 | 219 | 149 | 165 | 224 | 95 | 40 | 246 | 155 |
| $\sigma(R_{4.945})$ | 41 | 72 | 70 | 98 | 59 | 28 | 26 | 26 | 29 | 87 | 48 | 28 | 6 |
| $R_{5.11}$ | 0 | 0 | 0 | 533 | 0 | 238 | 0 | 0 | 0 | 0 | 0 | 0 | 0 |
| $\sigma(R_{5.11})$ | 0 | 0 | 0 | 54 | 0 | 71 | 0 | 0 | 0 | 0 | 0 | 0 | 0 |
| $R_{6.128}$ | 0 | 0 | 0 | 838 | 0 | 436 | 0 | 250 | 0 | 0 | 0 | 0 | 0 |
| $\sigma(R_{6.128})$ | 0 | 0 | 0 | 85 | 0 | 73 | 0 | 75 | 0 | 0 | 0 | 0 | 0 |

**Table 4.21.** October 3, 2007 Figures-of-Merit Using Fert30 as Template

| Sample | $\varsigma$ | $\sigma(\varsigma)$ |
|---|---|---|
| Air | 6787.405 | 12.836 |
| Aluminum | 1461.943 | 8.745 |
| Antifreeze | 54.016 | 3.834 |
| Paint | 13.300 | 2.701 |
| Chalk | 548.055 | 6.843 |
| Fertilizer 30% | 0.000 | 0.000 |
| Fertilizer 36% | 90.760 | 4.365 |
| Fertilizer Mix | 25.156 | 3.167 |
| Polyethylene | 106.896 | 4.547 |
| Rubber | 76.074 | 4.177 |
| Sand | 350.714 | 6.120 |
| Washer Fluid | 419.734 | 6.401 |
| Water | 134.489 | 4.816 |

**Table 4.22.** October 3, 2007 Figures-of-Merit Using Fert 36 as Template

| Sample | $\varsigma$ | $\sigma(\varsigma)$ |
|---|---|---|
| Air | 8429.874 | 13.551 |
| Aluminum | 2278.584 | 9.821 |
| Antifreeze | 110.774 | 4.588 |
| Paint | 87.679 | 4.327 |
| Chalk | 1259.661 | 8.425 |
| Fertilizer 30% | 90.760 | 4.365 |
| Fertilizer 36% | 0.000 | 0.000 |
| Fertilizer Mix | 102.562 | 4.501 |
| Polyethylene | 125.094 | 4.834 |
| Rubber | 5.661 | 2.182 |
| Sand | 710.550 | 7.302 |
| Washer Fluid | 81.643 | 4.251 |
| Water | 162.468 | 5.049 |

**Table 4.23.** October 3, 2007 Figures-of-Merit Using FertMix as Template

| Sample | $\varsigma$ | $\sigma(\varsigma)$ |
|---|---|---|
| Air | 6830.182 | 12.857 |
| Aluminum | 1462.510 | 8.747 |
| Antifreeze | 27.421 | 3.236 |
| Paint | 47.203 | 3.707 |
| Chalk | 711.563 | 7.304 |
| Fertilizer 30% | 25.156 | 3.167 |
| Fertilizer 36% | 102.562 | 4.501 |
| Fertilizer Mix | 0.000 | 0.000 |
| Polyethylene | 99.726 | 4.496 |
| Rubber | 81.942 | 4.255 |
| Sand | 285.141 | 5.811 |
| Washer Fluid | 480.482 | 6.621 |
| Water | 145.181 | 4.909 |

# Chapter 5

# Conclusions and Recommendations

## 5.1 Conclusions

The template matching technique for detection of explosive materials holds much promise. It has been shown that the method can distinguish explosive surrogates from inert materials when interrogated with neutrons. Samples of various sizes at a distances greater than a meter were able to be identified as an explosive or non-explosive.

## 5.2 Recommendations

Further experimentation is still necessary to optimize this system. This should include experimentation at various distances, experimentation with clutter, and experimentation with different actual or simulated explosives. It is also recommended that these results in this thesis and future experimentation be used to determine appropriate values of $\alpha_i$ (weight factors) for each energy "i." In addition, experimentation with a neutron generator is necessary to make the system portable. The system should also be automated to perform the interrogation, analysis, and give a positive or negative result with the click of a button. Once these steps are complete, a template library can be created.

## 5.3 Additional Applications

Since the determination of the elements within an object is based upon comparison of signatures, this device could be used in a vast number of applications. It could be employed

for quality control of foods or chemicals to ensure they are the appropriate composition. It could be used to find illicit drugs or nuclear materials. Scientists could use it to test imported goods for lead paint. The possibilities for its uses are endless.

# Bibliography

[1] Analysis Defense Manpower Data Center Data and Programs Division. Dod personnel and military casualty statistics, defense manpower data center, casualty summary by reason, October 7, 2001 through April 4, 2009. Technical report, 2009. available at [http://siadapp.dmdc.osd.mil/personnel/CASUALTY/gwot_reason.pdf].

[2] E.L. Reber, L.G. Blackwood, A.J. Edwards, J.K. Jewell, K.W. Rhode, E.H. Seabury, and J.B. Klinger. Idaho explosives detection system. *Nuclear Instruments and Methods in Physics Research B*, 241:738–742, 2005.

[3] P. Machler. Detection technologies for anti-personnel mines. In *Symposium on Autonomous Vehicles in Mine Countermeasures*, Moterey, 1995.

[4] A. Buffler. Contraband detection by fast neutron scattering. In *Proceedings of the 2nd National Nuclear Technology Conference*, South Africa, 2001. Paper No. D-O3.

[5] A. Buffler. Contraband detection with fast neutrons. *Radiation Physics and Chemistry*, 71:853–861, 2004.

[6] E.M.A. Hussein and E.J. Waller. Review of one-sided approaches to radiographic imaging for detection of explosives and narcotics. *Radiation Measurements*, 29:581–591, 1998.

[7] A.J. Caffrey, J.P. Cole, R.J. Gehrke, and R.C. Greenwood. Chemical warfare agent and high explosive identification by spectroscopy of neutron-induced gamma rays. *IEEE Transactions on Nuclear Science*, 39:1422–1426, 1992.

[8] K.P. Hong, C.M. Sim, V. Em, S.W. Lee, Y.J. Kim, S.Y. Park, J.Park, and H.J. Kim. Comparison with existing interrogation system technologies for explosives. In *Proceed-*

*ings of the International Symposium on Research Reactor and Neutron Science*, Daejeon, Korea, 2005.

[9] C. Bruschini. Commercial systems for the direct detection of explosives (for explosive ordnance disposal tasks). Technical report, Ecole Polytechnique Federale de Lausanne (EPFL) & Vrije Universiteit Brussel (VUB), 2001.

[10] Geneva International Centre for Humanitarian Demining. *Guidebook on Detection Technologies and systems for Humanitarian Demining*. 2006.

[11] G.M. Stone. Application and limitations of advanced technologies in explosives detection. *IEEE*, pages 81–87, 1990.

[12] S. Singh and M. Singh. Explosives detection system (EDS) for aviation security. *Signal Processing*, 83:31–55, 2003.

[13] *Existing and Potential Standoff Exposive Detection Techniques*. National Academy of Sciences, 2004.

[14] L. Thiesan, D. Hannum, D.W. Murray, and J.E. Parmeter. Survey of commercially available explosives detection technologies and equipment 2004. Technical report, U.S. Department of Justice, 2005. Document Number 208861.

[15] H. Strecker. Automatic detection of explosives in airline baggage using elastic x-ray scatter. *Medicamundi*, 42:30–33, 1998.

[16] A.A. Faust, J.E. McFee, H.R. Andrews, and H. Ing. Investigation of the feasibility of fast neutron analysis for detection of buried landmines. In J.T. Broach, R.S. Harmon, and H.H. Holloway, editors, *Detection and Remediation Technologies for Mines and Minelike Targes XI*, volume 6217. SPIE, 2006.

[17] G. Vourvopoulos. Accelerator based techniques for contraband detection. *Nuclear Instruments and Methods in Physics Research B*, 89:388–393, 1994.

[18] T. Gozani. Neutron based non-intrusive inspection techniques. In G. Vourvopoulus, editor, *Proceedings of the Fifth International Conference on Applications of Nuclear Techniques*, volume 2867, pages 174–181, Crete, Greece, 1997. SPIE.

[19] T. Gozani. Novel applications of fast neutron interrogation methods. *Nuclear Instruments and Methods in Physics Research A*, 353:635–640, 1994.

[20] B.J. Micklich, C.L. Fink, and T.J. Yule. Accelerator requirements for fast-neutron interrogation of luggage and cargo. In *Proceedings of the 1995 Particle Accelerator Conference*, Dallas, TX, 1995.

[21] R. Loveman, J. Bendham, T. Gozani, and J. Stevenson. Time of flight fast neutron radiography. *Nuclear Instruments and Methods in Physics Research B*, 99:765–768, 1995.

[22] C.L. Fink, P.G. Humm, M.M. Martin, and B.J. Micklich. Evaluation of few-view reconstruction parameter for illicit substance detection using fast-neutron transmission spectroscopy. *IEEE Transactions on Nuclear Science*, 43:1352–1356, 1996.

[23] F.D. Brooks, A. Buffler, M.S. Allie, K. Bharuth-Ram, M.R. Nchodu, and B.R.S. Simpson. Determination of HCNO concentrations by fast neutron scattering analysis. *Nuclear Instruments and Methods in Physics Research A*, 410:319–328, 1998.

[24] A. Buffler, F.D. Brooks, M.S. Allie, K. Bharuth-Ram, and M.R. Nchodu. Material classification by fast neutron scattering. *Nuclear Instruments and Methods in Physics Research B*, 173:483–502, 2001.

[25] G. Vourvopoulos. Pulsed fast/thermal neturon analysis: A technique for explosive detection. *Talanta*, 54:459–468, 2001.

[26] G. Nebbia. The use of tagged 14 MeV neutron beams for the detection of illicit materials in land and sea transportation. In *2005 IEEE Nuclear Science Symposium Conference Record*, pages 134–137, Puerto Rico, 2005. IEEE.

[27] Victor Bom and C.W.E. van Eijk. Using the method of neutron back scattering imaging to detect hidden explosives. In *2005 IEEE Nuclear Science Symposium Conference Record*, pages 138–142, Puerto Rico, 2005. IEEE.

[28] C. Datema, V.R. Bon, and C.W.E. van Eijk. DUNBLAD, the delft university neutron backscattering landmine detector. In *Proceedings of the fifth International Symposium on Technology and the Mine Problem*, 2002.

[29] F.D. Brooks, A. Buffler, and M.S. Allie. Detection of anti-personnel landmines using neutrons and gamma-rays. *Radiation Physics and Chemistry*, 71:749–757, 2004.

[30] E. Rhodes, C.E. Dickerman, A. DeVolpi, and C.W. Peters. APSTNG: Radiation interrogation for verification of chemical and nuclear weapons. *IEEE Transactions on Nuclear Science*, 39:1041–1045, 1992.

[31] J.A. Bamberger, R.A. Craig, T.Y. Colgan, A.J. Peurrung, B.E. Schmitt, and D.C. Stromswold. Time-neutron detection for landmines. *IEEE*, pages 1336–1340, 2004.

[32] T. Cousins, T.A. Jones, J.R. Brisson, J.E. McFee, T.J. Jamieson, E.J. Waller, F.J. LeMay, H. Ing, E.T.H. Clifford, and E.B. Selkirk. The development of a thermal neutron activation (TNA) system as a confirmatory non-metallic land mine detector. *Journal of Radioanalytical and Nuclear Chemistry*, 235:53–58, 1998.

[33] Thermal neutron activation (TNA) for non-metallic land mine detection, 2004. Fact Sheet.

[34] P.C. Womble, G. Vourvopoulos, J. Paschal, I. Novikov, and A. Barzilov. Results of field trials for the PELAN system. In *Proceedings of the SPIE*, volume 4786, pages 52–57, 2002.

[35] P.C. Womble, G. Vourvopoulos, and J. Paschal. Detection of landmines using the PELAN system. 2001.

[36] A. Chalmers. Rapid inspection of cargos at portals using drive-through transmission and backscatter x-ray imaging. In *Proceedings of SPIE*, volume 5403, 2004.

[37] F.D. Brooks and M. Drosg. The HYDAD-D antipersonnel landmine detector. *Applied Radiation and Isotopes*, 63:565–574, 2005.

[38] William L. Dunn, K. Banerjee, Austin Allen, and Joshua Wayne Van Meter. Feasibility of a method to identify targets that are likely to contain conventional explosives. *Nuclear Instruments and Methods in Physics Research B*, 263:179–182, 2007.

[39] Kansas State University Department of Mechanical and Nuclear Engineering. *General Characteristics of the KSU TRIGA Mark II Reactor*.